Kv1.3 blockade Inhibits Proliferation of Vascular Smooth Muscle Cells In Vitro and Intimal Hyperplasia In Vivo

Joaquim Bobi, DVM[1*]; Manel Garabito, PhD[1*]; Núria Solanes, DVM, PhD[1*]; Pilar Cidad, PhD[2]; Víctor Ramos-Pérez, PhD[3]; Alberto Ponce, PhD[3]; Montserrat Rigol, DVM, PhD[1]; Xavier Freixa, MD, PhD[1]; Claudia Pérez-Martínez, DVM, PhD[4]; Armando Pérez de Prado, MD, PhD[4]; Felipe Fernández-Vázquez, MD, PhD[4]; Manel Sabaté, MD, PhD[1]; Salvador Borrós, PhD[3,5]; José Ramón López-López, MD, PhD[2]; Mª Teresa Pérez-García, MD, PhD[2**]; Mercè Roqué, MD, PhD[1**].

1) Institut d'Investigacions Biomédiques August Pi i Sunyer (IDIBAPS) and Cardiology Department, Institut Clínic Cardiovascular, Hospital Clínic, Universitat de Barcelona, Barcelona, Spain. 2) Departamento de Bioquímica y Biología Molecular y Fisiología and Instituto de Biología y Genética Molecular (IBGM), Universidad de Valladolid and CSIC, Valladolid, Spain. 3) Grup d'Enginyeria de Materials (GEMAT), Institut Químic de Sarrià (IQS), Universitat Ramon Llull (URL), Barcelona, Spain. 4) Grupo Cardiovascular (HemoLeon), Fundación Investigación Sanitaria en León y del Instituto de Biomedicina (IBIOMED), Universidad de León, Hospital Universitario de León, León, Spain. 5) CIBER of Biomaterials Bioengineering and Nanomedicine (CIBER-BBN), Barcelona, Spain.

* These authors contributed equally to this work.

**Both senior authors contributed equally to the study.

Correspondence to: Mercè Roqué, Institut Clínic Cardiovascular, Hospital Clínic de Barcelona. Villarroel 170, 08036 Barcelona, Spain. e-mail: mroque@clinic.cat

Running Head: Kv Channels Modulation to Prevent Intimal Hyperplasia

Abbreviations: AV, allograft vasculopathy; ISR, in-stent restenosis; Kv channel, voltage-gated K^+ channel; PAP-1, 5-(4-phenoxybutoxy)psoralen; PM, phenotypic modulation; VSMCs, vascular smooth muscle cells.

Abstract

The modulation of voltage-gated K^+ (Kv) channels, involved in cell proliferation, arises as a potential therapeutic approach for the prevention of intimal hyperplasia present in in-stent restenosis (ISR) and allograft vasculopathy (AV). We studied the effect of PAP-1, a selective blocker of Kv1.3 channels, on development of intimal hyperplasia *in vitro* and *in vivo* in two porcine models of vascular injury. *In vitro* phenotypic modulation of VSMCs was associated to an increased functional expression of Kv1.3 channels, and only selective Kv1.3 channel blockers were able to inhibit porcine VSMC proliferation. The therapeutic potential of PAP-1 was then evaluated *in vivo* in swine models of ISR and AV. At 15-days follow-up, morphometric analysis demonstrated a substantial reduction of luminal stenosis in the allografts treated with PAP-1 (autograft 2.72±1.79 vs allograft 10.32±1.92 vs allograft+polymer 13.54±8.59 vs allograft+polymer+PAP-1 3.06±1.08 % of luminal stenosis; P=0.006) in the swine model of femoral artery transplant. In the pig model of coronary ISR, using a prototype of PAP-1-eluting stent, no differences were observed regarding % of stenosis compared to control stents (31±13 % vs 37±18%, respectively; P=0.372) at 28-days follow-up. PAP-1 treatment was safe and did not impair vascular healing in terms of delayed endothelialization, inflammation or thrombosis. However, an incomplete release of PAP-1 from stents was documented. We conclude that the use of selective Kv1.3 blockers represents a promising therapeutic approach for the prevention of intimal hyperplasia in AV, although further studies to improve their delivery method are needed to elucidate its potential in ISR.

Introduction

Vascular wall remodeling and intimal hyperplasia is a pathological process common to a number of highly prevalent cardiovascular entities, which critically influences patient outcomes. Upon vascular injury, there is a cascade of signaling events, ultimately leading to the process known as phenotypic modulation (PM), which involves the switch of the vascular smooth muscle cells (VSMCs) from a contractile to a proliferative phenotype. This switch will have an influence on vascular structure, function and tone. VSMCs on the vessel wall undergo this PM, characterized by migration, proliferation, loss of contractile proteins and enhanced synthesis of extracellular matrix. Migration and proliferation of VSMCs are the central steps in response-to-injury and vascular remodeling leading to development of intimal hyperplasia.[1–4]

Intimal hyperplasia is a prominent feature of allograft vasculopathy (AV) and in-stent restenosis (ISR), two clinical entities with a high socio-economic relevance. Chronic AV is characterized by diffuse intimal hyperplasia formation and negative vascular remodeling leading to a progressive luminal narrowing which, in late stages, can result in a critical stenosis and graft ischemia and malfunction.[5–7] AV remains as a major limitation to the long-term success of solid organ transplantation[6]. Similarly, ISR is widely recognized as an independent predictor of mortality after stent implantation.[8] The use of drug eluting stents (DES) delivering antiproliferative compounds, such as everolimus, sirolimus, paclitaxel and zotarolimus, among others, have made a major impact in ISR reduction.[9,10] However, these drugs are not specific for VSMCs, inhibiting proliferation of all cell types in the vessel wall, including endothelial cells. As a consequence, an increased incidence of late in-stent thrombosis, due to delayed reendothelialization has been reported,[8] and the availability of new compounds with a more selective mechanism of action would make a significant clinical difference.

The search for novel therapies against restenosis is a very active field of research, which has been hampered by our limited knowledge of the mechanisms of PM of VSMC. One important regulator involved in VSMC proliferation are ion channels.[4,11,12] Among those, voltage-gated K^+ channels (Kv channels) have been described to be implicated in cell proliferation in different preparations.[13,14] Our group has previously demonstrated that Kv1.3, a voltage-dependent K^+

channel, is involved in VSMC PM in response to vascular injury *in vitro* , as well as *in vivo*,[15–17] and the selective blockade, by 5-(4-phenoxybutoxy)psoralen (PAP-1), has promising therapeutic potential in a small-animal model of endovascular injury.[17]

For translational purposes, in order to extrapolate these results to a scenario closer to clinical practice, species and/or vascular bed specific differences must be ruled out. Here, we analyze the efficacy of PAP-1 treatment both *in vitro* and in two clinically-relevant large animal models of AV and ISR.

Methods

This study was conducted following the European Directive 2010/63/UE and Spanish RD 53/2013 regulations related to the Guide for the Care and Use of Laboratory Animals. Protocols were approved by the Animal Experimentation Ethics Committee of the University of Barcelona (approval reference number: DAAM 5605 and 8574/9319).

Study design

The antiproliferative capacity of PAP-1 on smooth muscle cells was first studied *in vitro* and compared to landmark potassium-channel blocker drugs. A polymer-based strategy was designed and tested *in vitro* for the delivery of PAP-1 in the swine models of vascular injury. In total, 31 Large-White x Landrace female pigs were used in this study to test the effect of PAP-1 on intimal proliferation after arterial allograft transplantation, balloon injury, and coronary stenting (**Figure 1**). In the femoral artery transplant model, grafts were treated with the polymer carrying PAP-1 or naïve, and animals were followed for 15 days. In parallel, in the coronary ISR model, coronary arteries were stented with polymer-coated stents with or without PAP-1 and harvested 28 days after stenting. In both models, animals were randomly allocated to the different study groups.

Collection of injured coronary vascular samples, cell dissociation and culture

Coronary arteries were *in vivo* injured in two female pigs for molecular, *in vitro* electrophysiological and cell culture studies. Circumflex and anterior descendent coronary arteries underwent angioplasty balloon injury (balloon-to-artery ratio of 1.1-1.3). Right coronary arteries were used as controls. At 4 weeks follow-up, animals were euthanized, and coronary

vessels were harvested under aseptic conditions for molecular, cell culture and electrophysiology assays. Arteries were divided in two pieces, one of which was placed in RNAlater (Ambion) for RNA extractions and the other in a Dulbecco's modified Eagle's medium (DMEM), for cell isolation. Both samples were kept at 4º C and transported from Barcelona to Valladolid within the next 24 hours following intervention.

VSMCs were isolated from the medial layer of the vessel kept in DMEM after manual removal of both adventitia and endothelial layers under a dissection microscope. Once isolated, the muscle layer was cut into 1-3 mm pieces. Some of these pieces were used for obtaining acute dispersed cells for patch-clamp experiments (see below) , and some were placed in 35 mm Petri dishes treated with 2 % gelatine (Type B from bovine skin, Sigma) or collagen (6 well multidish collagen, Thermo Scientific), in DMEM supplemented with 20 % SFB, penicillin-streptomycin (100 U/ml each), 5 µg/ml fungizone, and 2 mM L-glutamine (Lonza) at 37 ºC in a 5 % CO2 humidified atmosphere. Migration and proliferation of VSMCs from the explants was evident within 10-15 days. Confluent cells were trypsinized and seeded at 1/3 density and VSMCs were subjected to several (up to 8) passages in control medium. The composition of this media was DMEM with 5 % FBS, penicillin-streptomycin, fungizone and L-glutamine as above, and supplemented with 5 µg/ml Insulin, 2 ng/ml bFGF and 5 ng/ml EGF.

To obtain fresh dispersed VSMCs, the small pieces of endothelium-free coronary artery were placed at 4 ºC for 30 min in PBS(-) (nominally Ca2+- and Mg2+-free PBS solution with 5 mM glucose) containing 0.2-0.1 % collagenase IV and 0.1% BSA (Sigma) and then incubated at 37 ºC for 5-10 min in a shaking water bath. At the end of this first incubation, tissues were washed twice in PBS (-) solution and additionally incubated during 20 min in a 0.2-0.1 % collagenase IV and 0.1-0.05 % trypsin (Sigma) PBS (-) solution. After washing of this second incubation, single cells were obtained by gentle trituration with a wide-bore glass pipette. Dispersed cells were stored in PBS at 4º C, to be used within the same day.

For the isolation of VSMCs from injured arteries, a different dissociation protocol was employed, based on a previously described method.[18] Briefly, after careful dissection of connective tissue, small pieces of artery were placed in 200 µL of culture media (D-MEM

medium supplemented with 10 % FBS, penicillin-streptomycin (100 U/ml each), 5 µg/ml fungizone and 2 mM L-glutamine) containing 1.36 mg/ml collagenase type I (Worthington), and left in the incubator (at 37 ºC in a 5 % CO2 humidified atmosphere) for four to six hours. After that, 3 ml of culture media were added and cells were transferred to a conical tube and centrifuged for 5 min at 300xg. The pellet was resuspended in a small volume of culture medium and dispersed cells were plated onto poly-L-lysine coated coverslips with 2ml of culture medium supplemented with 1 % FBS and maintained in the incubator. Electrophysiological experiments were performed within 4-24 hours after isolation. Parallel studies using this dissociation method were performed with VSMCs isolated from contralateral control arteries to confirm that the differences in the isolation and culture conditions did not modify the expression pattern of ion channels observed in acutely dispersed VSMCs.

RNA expression of Kv1.3 and Kv1.5

The samples stored in RNAlater™ were homogenized with a handheld homogenizer (Omni International Inc.). RNA from the tissue homogenates and from cultured VSMCs was isolated with TRIzol Reagent and reverse transcribed as previously described.[16] The mRNA levels of Kv1.3 (Kcna3)), Kv1.5 (Kcna5) and Glyceraldehyde 3-phosphate dehydrogenase (Gapdh) were determined by real-time qPCR using SybrGreen (for Gapdh) or Taqman® probes (for Kcna3 and Kcna5) on a Rotor-Gene 3000 instrument (Corbett Research) using the $2^{-\Delta\Delta Ct}$ relative quantification method.[19] mRNA expression levels were normalized to the internal control, Gapdh mRNA. The relative abundance of the genes was calculated from $2^{(-\Delta Ct)}$, where $\Delta Ct = Ctgene - CtGapdh$ and the changes in expression between the different experimental conditions were calculated from $2^{(-\Delta\Delta Ct)}$, where $\Delta\Delta Ct = \Delta Ct(experimental) - \Delta Ct(control)$, the calibrator sample is indicated in each case. In this way, data in the different experimental conditions are presented as the fold change in gene expression. For the representation of these data, the logarithm of $2^{-\Delta\Delta Ct}$ was used, so that a value of 0 means no change, positive values represent increased expression and negative values decreased expression. Total RNA from human brain (BD Biosciences) was used as positive control. Primers sets employed are listed in Supplemental table 1.

VSMCs electrophysiological studies

Ionic currents were recorded at room temperature (20-25 ºC) using the whole-cell configuration of the patch-clamp technique. Whole-cell current recordings and data acquisition from VSMC cells were made as previously described.[20] Briefly, the coverslips with the attached VSMCs in culture (or the freshly dispersed VSMCs) were placed at the bottom of a small recording chamber on the stage of an inverted microscope and perfused by gravity with an external solution of the following composition (in mM): 141 NaCl, 4.7 KCl, 1.2 MgCl2, 1.8 CaCl2, 10 glucose, 10 HEPES, pH 7.4 (with NaOH). Paxilline (0.5 µM), and Tetrodotoxin (0.1 µM) were included in the bath solution to block large conductance Ca2+-dependent K+ channels and voltage-activated Na+ channels respectively. When freshly isolated VSMCs were used, they were placed directly in the recording chamber and allowed to settle for a few minutes before starting perfusion with the external solution. Patch pipettes were made from borosilicate glass (2.0 mm O.D., WPI) and double pulled (Narishige PP-83) to resistances ranging from 4 to 8 MΩ when filled with the internal solution, containing (in mM): 125 KCl, 4 MgCl2, 10 HEPES, 10 EGTA, 5 MgATP; pH 7.2 with KOH.

Whole-cell currents were recorded using an Axopatch 200 patch-clamp amplifier, filtered at 2 kHz (-3 dB, 4-pole Bessel filter), and sampled at 10 kHz. When leak-subtraction was performed, an online P/4 protocol was used. Series resistance was routinely compensated. Recordings were digitized with a Digidata 1200 A/D interface, driven by CLAMPEX 8 software (Axon Instruments) in a PC computer. K channel blockers Margatoxin (MgTx) and Paxiline (Pax) were acquired form Alomone (Alomone Labs) and PAP-1 was purchased from Sigma. Electrophysiological data analyses were performed with the CLAMPFIT subroutine of the PCLAMP software (Axon) and with ORIGIN 7.5 software.

VMSCs migration assay

To evaluate migration, we used a wound healing or scratch assay,[16] in cultured VSMCs. Cells were seeded in 4-well plates (1.8 cm^2/well) and grown in SMC-P-STIM medium until confluence. Monolayers were manually scraped with a 200 µL pipette tip, gently washed three times with PBS to remove non-adherent cells and incubated in a serum free medium (SF

medium) to block proliferation. The SF medium is a DMEM supplemented with 500 nM insulin, 5 µg/ml transferrin 100 U/ml each penicillin and streptomycin, 5 µg/ml fungizone, and 2 mM L-glutamine. Images of the scratched area were taken immediately (time 0) and 24 hours after injury. The scratched area was measured using Image J software. Percentage of invaded area was determined as: % Reinvasion = [(Area0-Area24)/Area0] x 100, where Area0= initial area (t=0) and Area24 = area at time 24 h after injury. Migration assays were performed in drug-free conditions (control) or presence of 100 nM PAP-1, and 1 or 0.1 nM Everolimus (Sigma).

VMSCs proliferation assays

Pig coronary cultured VSMCs were plated in poli-L-lysine coated coverslips and grown to approximately 65-80 % confluence. At this point, cells were synchronized by incubation during 48-72 hours in SF medium at 37 ºC in a 5% CO2 humidified atmosphere. After this, cells were either maintained in SF medium (negative control), placed in SMC-P-STIM medium alone (control) or SMC-P-STIM medium with 5 µM Correolide, 50 nM Stromatoxin (Alomone Labs), 100 µM TEA (Sigma), 10 nM Margatoxin or 100 nM PAP-1, (experimental conditions) during 24 hours. At the end of this period, BrdU incorporation assay were performed by incubation with the BrdU labeling medium for 60 min at 37 ºC in a 5% CO2 humidified atmosphere and then fixed with 50 mM glycine solution in 70% ethanol for 20 min at -20 ºC. Incorporated BrdU was detected by 30 min incubation at 37ºC with anti-BrdU, followed by 30 min incubation at 37ºC with anti-mouse-Ig-fluorescein, according to manufacturer's instructions (Roche Applied Science, Germany). Coverslips were mounted in Vectashield with DAPI (Vector Laboratories, INC., Burlingame, CA), and BrdU incorporation was measured and represented as the percentage of BrdU positive nuclei (BrdU+) from the total nuclei number stained with DAPI. In each experiment, BrdU incorporation was obtained from the average of at least 10 different fields for each condition.

Femoral artery transplant model

A total of 16 pigs (9 recipients, 7 donors; 33.2 ± 4.3 kg) were used. Femoral artery transplantation was carried out following the surgical technique previously described.[21,22] The animals were anesthetized with propofol (10 mg/kg per hours, IV) and fentanyl (0.005–0.01

mg/kg per hour, IV), treated with analgesia (buprenorphine 0.3 mg, IM after weaning) and ventilated as previously described.[23] Intravenous cefoxitin (30 mg/kg) was administered as antibiotic prophylaxis. Inyesprin (300 mg) as anti-platelet therapy and heparin (first dose of 4000 UI before clamping the artery, followed by of 1000 UI 1hour after the first dose) as anti-coagulant therapy were also administered intravenously during surgery. Animals were randomly assigned to be femoral artery donors or recipients. In order to avoid any possible systemic effect of PAP-1, recipient animals were distributed in three subgroups: animals with an untreated autograft in the right femoral artery and an untreated allograft in the left femoral artery (n=4); animals with polymer treated allografts in both femoral arteries (n=2); or animals with polymer+PAP-1 treated allografts in both femoral arteries (n=3). Briefly, femoral arteries from recipient pigs were dissected and a segment excised from each artery. An allograft or an autograft were implanted by means of an end-to-end anastomosis. Autografts were obtained by replacing a left femoral artery segment with the right femoral artery segment from the same animal and used as control grafts. Femoral segments were maintained in a 5% glucose solution (Glucose 5%, Baxter SL, Valencia, Spain) at 37 °C until implantation. Prior to closing the surgical wound, grafts were left untreated, treated with polymer (PLGA 50/50) alone or with PAP-1 (1 μg/mm^2). Eighteen grafts were harvested and resulted in the following: control autografts (n=4); control allografts (n=4); allografts treated with the isolated polymer (n=4); and allografts treated with the polymer carrying PAP-1 (n=6). Fifteen days after surgery, animals were anesthetized and *in vivo* graft patency was assessed by angiography. Thereafter, animals were euthanized by anesthesia overdose of sodic thiopental (2g, IV). The femoral arteries were perfused-fixed with phosphate-buffered saline (PBS) and 10% neutral buffered formalin and harvested with the margins of the native artery at both ends for further histologic and morphometric analysis.

Histology and morphometry of femoral arterial grafts

Histological procedures and analytical methods were performed as previously described.[21,22] In summary, histological sections were stained with hematoxylin eosin to describe vascular lesions. Morphometric analyses were performed on histological sections obtained from the

middle of the grafts. These sections were stained by orcein and Verhoeff Van Gieson to identify elastic fibers. The analyses of morphometric graft parameters were done using the MicroImage software (Olympus Optical, Hamburg, Germany).

Porcine Model of Coronary in-Stent-Restenosis

Thirteen pigs (30.2±1.7 kg) underwent a percutaneous coronary intervention to stent each one of the main coronary arteries. The drug-eluting stent prototypes were designed to obtain a secure, long-lasting stent with a controlled burst effect by using two different polymers: a more hydrophobic polymer (PLGA) and a more hydrophilic one (pHPMA) for allowing burst release. The animals were anesthetized, treated with analgesia and ventilated as described above. Radiopaque contrast (Iomeprol 350 mg/ml, Iomeron 350, Bracco, Wycombe, UK) was administered to obtain coronary angiographies, which were used to screen for appropriate vessel segments for stent implantation on the basis of anatomy and the diameter (between 2.3 and 3.0 mm) measured in situ on a fluoroscope console (Arcadis Avantic, Siemens AG, Germany). Briefly, polymer-coated, with (n=18) or without (n=18) PAP-1, stents of 3 mm in diameter and 23 mm of length were percutaneously implanted in the selected coronary segments. For stent deployment, angiographic contrast was used to inflate balloon at 7 to 15 atmospheres (2.97-3.37 mm) for 10 seconds to achieve a at a stent-to-artery ratio (SAR) of 1.1-1.3. Only stents from the same treatment (with or without PAP-1) were implanted in each animal (control group, n=6; PAP-1 group, n=7) and only coronary arteries with a diameter suitable for the aimed SAR were stented. Two left anterior descending coronary arteries from PAP-1 animals resulted too small for the desired SAR. Thus, one more animal was included in the PAP-1 group, in which the left anterior descending and circumflex coronary arteries were stented. After angiographic confirmation of correct stent deployment, animals were awakened and weaned from mechanical ventilation. Dual anti-platelet therapy was continued with 200 mg aspirin and 75 mg clopidogrel until the end of follow-up. At 28 days follow-up, after coronary angiography to study the patency of stented coronary segments, animals were euthanized by anesthesia overdose of sodic thiopental (2g, IV). The hearts were excised, coronary arteries were pressure-perfused with

saline (0.9% NaCl) and then fixed with 10 % neutral buffered formalin for 7 days. The stented coronary segments were carefully dissected, preserving at least 5 mm proximally and distally. Detailed methods of the design and optimization of the Polymer-Coated Drug-Eluting Stent Prototypes are described in **Supplemental Methods.**

Histology and morphometry of stented coronary segments

The stented arteries were embedded in resin plastinated casts in order to take representative circumferential sections of the proximal, mid and distal segments of each sample, and to calculate mean values for each studied segment. After deplastinating the sections, we performed routine hematoxylin-eosin and Verhoeff Van Gieson elastic staining procedures.

The arteries were analyzed histomorphometrically by a pathologist blinded to study design, with digital microscopy imaging using an Olympus PRovis AX70® (Tokyo, Japan) with a Nikon DXM 1200® digital camera and the software ImageJ-NIH Image 1.4 (National Institutes of Health, United States). We used planimetry to determine the luminal and internal elastic lamina areas and calculate the 2 restenosis variables defined by histology:

- Neointimal area = internal elastic lamina area – luminal area
- Histologic percent diameter stenosis = [1 – (luminal area/internal elastic lamina area)] × 100.

The histopathologic analysis of treatment safety was based on the semiquantitative analysis of the 4 main parameters:[24] injury score,[25] inflammatory severity,[26] persistent fibrin[27] and degree of re-endothelialization. Endothelial coverage was semi-quantified and expressed as an estimated percentage of the lumen circumference.

After histologic assessments were undertaken, the remaining levels of PAP-1 in the implanted stents were analyzed by HPLC–Ultraviolet and confirmed by HPLC-Mass Spectrometry in segments of approximately 8 mm in length. The initial PAP-1 absolute concentration in the drug-eluting stents was estimated to be 100 μg.

Statistical analysis

Statistical analysis was performed using SPSS software (IBM SPSS Statistics for Windows, Version 23.0, released 2013; IBM Corp, Armonk, NY) and GraphPad Prism (version 5.00 for

Windows; GraphPad Software, San Diego, CA) was used to create graphics dots. Continuous normal distributed variables *in vivo* and in *in vitro* experiments are represented as mean ± standard deviation (SD) or error of the mean (SEM), respectively. Differences among groups were studied with the t test in ISR model. Analysis of variance (ANOVA) and Bonferroni's post hoc tests were used to compare quantitative variables from AV model morphometric and VSMCs *in vitro* experiments data.

Results

Changes in Kv1.3 and Kv1.5 mRNA expression upon endoluminal injury of porcine coronary arteries.

The role of Kv1.3 and Kv1.5 in the PM of VSMCs that promotes intimal proliferation upon vascular injury was assessed *in vitro* by quantifying the expression of both channels in VSMCs from injured and non-injured porcine coronary arteries. The contribution of both Kv channels was further confirmed in functional *in vitro* assays (patch-clamp and cell migration and proliferation) using Kv-specific blockers (**Figure 1C**).

The mRNA levels of Kv1.3 and Kv1.5 in both phenotypes were measured by real time PCR with custom made Taqman® assays using Gapdh as endogenous control. **Figure 2A** shows the mRNA abundance of both Kv1.3 and Kv1.5 (normalized to Gapdh expression), obtained from healthy arteries (control A.), from injured arteries, but analyzing separately the area of macroscopic lesion from the surrounding region (lesion and no lesion), and from cultured VSMCs obtained from explants, as a model of fully dedifferentiated VSMCs. Vascular injury has opposite effects in the expression of both channels (increase of Kv1.3 and decrease of Kv1.5), with the most dramatic change observed in cultured pig coronary VSMCs, where Kv1.5 expression is undetectable. The changes in expression associated with PM are more evident when the expression data are normalized to the control arteries (i.e., contractile phenotype is used as calibrator), as shown in **Figure 2B** (left plot). PM associates with a marked decrease of Kv1.5 channels expression, while changes in Kv1.3 are more variable. Therefore, when using the ratio between the two channels (Kv1.3 to Kv1.5 ratio) there is a progressive increase of this ratio associated with a more dedifferentiated phenotype (**Figure 2B,** right plot).

Patch clamp experiments in the whole-cell configuration were used to characterize the presence and contribution of Kv1.3 currents to the total outward K currents recorded in freshly isolated cells from healthy arteries (**Figure 3A**), freshly isolated cells from injured arteries (**Figure 3B**) or cultured coronary VSMCs (**Figure 3C**). **Figure 3A** and **B** shows representative traces obtained in fresh VSMC from healthy and injured pig coronary arteries, by applying a family of depolarizing pulses from -60 to +80 mV. In both cases, the Kv component of the total outward current could be explored in the presence of 500 nM Paxiline to block the large conductance, Ca^{2+}-activated K^+ currents (BK currents). In the presence of Paxiline, there were no significant differences in the total Kv current amplitude in control and injured VSMCs. However, the Kv1.3 fraction of the current, (i.e., the current sensitive to either 10 nM MgTx or 100 nM PAP-1) was significantly larger in VSMCs from injured arteries compared to VSMCs from healthy ones (67.35 ± 1.80 % vs 12.82 ± 4.10 % of the current, respectively; see **Figure 3D**). This increased functional contribution of Kv1.3 currents was also observed in cultured VSMCs (**Figure 3C, D**). Pig coronary VSMCs in primary culture showed a reduced Kv current amplitude compared to freshly dispersed VSMCs (Kv current density at +40 mV was 20.54 ± 1.01 pA/pF in fresh VSMC versus 7.10 ± 0.51 pA/pF in cultured VSMC, data not shown); however, the fraction of the current carried by Kv1.3 represented almost half of this current in the cultured VSMCs.

Next, we analyzed the possible association of the increased functional expression of Kv1.3 currents in dedifferentiated cells with the proliferative phenotype. For that purpose, we studied the effect of Kv1.3 current blockade on the ability of cultured VSMCs to migrate and proliferate. Proliferation rate was determined by the number of BrdU+ cells (**Figure 4A**). As shown in the graph, fetal bovine serum (FBS)-induced proliferation was significantly decreased in the presence of selective Kv1.3 blockers (100nM PAP-1 or 10 nM MgTx) as well as upon application of the Kv1.x blocker Correolide (Corr, 5 µM). On contrast, proliferation was not affected by the use of other K^+ channel blockers such as the Kv2 blocker Stromatoxin (ScTx, 50 nM) or the Kv3 blocker TEA (100 µM). Migration was determined in confluent coronary VSMCs by a scratch migration assay. After 24 hours in serum-free medium alone (control) the

invaded area was significantly larger than in cells treated with 100 nM PAP-1. Also, the application of everolimus (a selective mTOR inhibitor) was able to reduce migration in a dose-dependent way (**Figure 4B**). Altogether these data indicated that the increased functional expression of Kv1.3 channels in dedifferentiated VSMCs contributes to the migratory and proliferative phenotype of these cells.

Effect of PAP-1 on Allograft Vasculopathy

The effect of PAP-1 on intimal proliferation formation characteristic of allograft vasculopathy was evaluated *in vivo* in the swine model of femoral artery transplantation (**Figure 1A**). Femoral grafts surgeries were completed without major incidences. Fifteen days after surgery, one untreated allograft was found occluded, and excluded from the histological analysis. The remaining 17 grafts were patent, assessed by angiography, at the end of the follow-up period and were included in the morphometric analysis. Morphometric data are summarized in **Table 1**.

Fifteen days after surgery, development of intimal hyperplasia was confirmed, with an intima-to-media ratio significantly higher in untreated and polymer-treated allografts, when compared to autografts. However, the allograft treatment with the PAP-1-eluting polymer completely abolished intimal proliferation compared to allograft control groups (untreated and polymer-treated). This was translated in a preserved luminal morphology of PAP-1-treated allografts, as the percentage of luminal stenosis was significantly reduced, compared with polymer-treated allografts (3.06±1.08 % vs 13.54±8.59 %; $p<0.05$) and similar to untreated autografts (3.06±1.08 % vs 2.72±1.79%, respectively; p=NS).Representative images of femoral arterial grafts from all groups are shown in **Figure 5A**.

Effect of PAP-1 on in-Stent Restenosis

A reproducible porcine model of ISR was used to test the therapeutic potential of a PAP-1-eluting stent prototype to prevent coronary intimal proliferation (**Figure 1B**). Ten animals (Control, n=5; PAP-1, n=5) completed the follow-up, and coronary angiography at 28 days showed preserved patency of all stented coronary segments. Three animals (Control, n=1; PAP-1, n=2) died during the first 48 hours after intervention (necropsy was performed, and patency

of stented coronary arteries was confirmed; death was attributed to a respiratory infection). From the surviving animals, a total of 27 stented coronary segments (Control, n=15; PAP-1, n=12) were harvested and analyzed. Morphometric data of stented coronary arteries are summarized in **Table 2**, and representative photomicrographs of both groups are illustrated in **Figure 5B**. In summary, implantation of PAP-1-eluting stents did not result in a statistically significant decrease of intimal proliferation in the coronary arteries, compared to polymer alone-coated stents, although a mild tendency towards a decreased intimal proliferation was observed. Data from the safety assessment revealed that PAP-1 did not impair reendothelialization, which was complete, with 100 % of endothelial lining recovered at 28 days after coronary intervention. Inflammatory cells presence and fibrin deposition were very scarce and in a similar degree in both control and treatment groups. Furthermore, there was no evidence of occlusive or residual thrombosis in any of the stented coronary segments analyzed.

The assessment of the remaining PAP-1 in the stent prototypes by HPLC showed an incomplete release of the drug. An average concentration of 13.5 µg of PAP-1 was detected in the segments of the stent analyzed (data not shown), which can be extrapolated to an approximate amount of 40-45 µg of PAP-1 not having been released.

Discussion

In this study, we used a large, clinically-relevant, animal model to demonstrate that the increased functional expression of Kv1.3 channels associates with the PM of VSMCs, representing a promising target for the prevention of unwanted vascular remodeling. We found that selective Kv1.3 channel blockade with PAP-1 is able to inhibit migration and proliferation of cultured coronary VSMCs *in vitro,* and abolished intimal proliferation in an *in vivo* model of allograft vasculopathy **(Figure 6)**.

Kv1.3/Kv1.5 expression ratio has been proposed as a landmark of the VSMC phenotype, as it markedly increases with PM in all vascular territories studied.[4,28,29] Here, we confirm this observation in a new preparation. We found a gradual increase of the Kv1.3/Kv1.5 ratio from contractile VSMC tissue to cultured VSMC. We also confirm in this model that the changes in mRNA expression parallel changes in the functional contribution of the channel protein, as

there is an upregulation of Kv1.3 currents in dedifferentiated VSMCs. Moreover, although the total currents obtained in VSMCs from control or injured arteries are suggestive of changes in many other K^+ conductances, only the changes in Kv1.3 currents seemed to be related to the proliferative phenotype, as FBS-induced proliferation of VSMCs was selectively inhibited with Kv1.3 blockers. Using human vessels (mammary arteries and saphenous veins) in organ culture, we have recently demonstrated that also in this preparation inhibition of Kv1.3 channels can prevent unwanted remodeling and, in addition, we provide evidence suggesting that MYOCD-dependent expression of Kv1.5 channels, via modulation of the Kv1.3/Kv1.5 ratio in VSMCs, underlies the changes in the functional contribution of Kv1.3 channels to PM.[30] In this way, reduction of Kv1.5 in dedifferentiated VSMCs uncovers Kv1.3-dependent signaling pathways leading to proliferation. The role of Kv1.3 in VSMC proliferation and its contribution to intimal hyperplasia formation is demonstrated in porcine coronary arteries, as shown previously in different human vascular beds, such as in coronary, uterine and renal arteries, mammary arteries and saphenous veins,[29,30] therefore confirming the pig as an adequate pre-clinical model to study the contribution of ion channels in cardiovascular disease.

In the present study, PAP-1 local treatment dramatically reduced allograft vasculopathy development 2 weeks after transplant in our previously validated femoral artery transplantation model, which is highly reproducible,[21,22] and has the same histological features of human allograft vasculopathy. The effect of Kv1.3 blockade with PAP-1 has been previously investigated in a rat aortic transplant model of allograft vasculopathy,[31] in which a mild reduction on luminal occlusion, but no significant reduction of intima/media ratio was observed. However, in this latter work, PAP-1 was administered systemically, whereas in our study treatment was administered by local delivery through a PAP-1-eluting polymer which covered the entire adventitial surface of the transplanted femoral artery segment. It is possible that a higher local concentration of PAP-1 was achieved in the vessel wall in our model, leading to an enhanced effect. Also, differences in response-to-injury and ion channel expression between the rat and pig species, can account for the different results of both studies.

We then pursued developing a drug-eluting stent to release PAP-1 to explore the effects on coronary in-stent restenosis in the porcine model. In this model, we have not been able to show the same beneficial effect of local delivery of PAP-1. Given the previous evidence in several *in vitro* and *in vivo* studies,[16,17,29] we would have expected a reduction of intimal proliferation. Although a tendency towards a lesser intimal area in the PAP-1 treatment group can be observed, no significant differences in the morphometric parameters analyzed have been demonstrated.

Several facts may be considered to explain these results. *In vivo* release conditions may have been different than those estimated *in vitro*, and the drug may not have been properly released. Supporting this point of view, we have analyzed the remaining PAP-1 concentration in the stented segments, which is approximately 40-50% of the initial concentration, therefore implying the release was not as complete as expected by the preliminary experiments of release profile analysis. Another possible explanation for the lack of effect is the limitation of PAP-1 concentration which could be incorporated into the polymer. In our *in vitro* assays, a maximum concentration of 1.5 $\mu g/mm^2$ could be achieved, ensuring an adequate electron microscopy structure of the coated stent. It is possible that higher concentrations of the study drug would have effectively reduced intimal proliferation. Although PAP-1 concentration administered in the *in vivo* transplant model was similar (estimated 1 $\mu g/mm^2$), the total amount of drug applied on the external arterial surface was higher (300 µg per artery). In addition, the PAP-1-releasing polymer was applied on top of the transplanted femoral artery covering all the adventitia, thus remaining on-site during the whole follow-up period, until sacrifice of the animals 4 weeks after. No release into the circulation was expected, therefore it is likely that the concentration of PAP-1 delivered to the arterial vessel wall was much higher than that delivered endoluminal by the PAP-1 eluting stent. Developing a drug-eluting stent is technically a very demanding process. However, the high manufacturing cost of PAP-1 and the fact that a local delivery approach seemed more adequate to the coronary intimal hyperplasia model for translational purposes, made us aim to develop a drug-eluting stent releasing PAP-1 in the vessel wall. Nonetheless, the intrinsic limitations of the swine model of ISR should also be considered when

interpreting the results of the PAP-1 stent prototype. To note, it is debated whether late vascular response (i.e., neointimal formation after 28 days) after DES implantation in swine models may or may not correlate with clinical restenosis or increased target legion revascularization in clinical trials out to 4 years long-term. And it has been suggested that long-term time points in pig model should be used for safety and biocompatibility assessment as they remain insufficiently validated for efficacy endpoints.[32] The polymer used in our stent has shown to have no side-effects, like excessive inflammation or fibrin deposition, as shown by the histological analysis. Also, there was no evidence of occlusive or residual thrombosis in any of the stented coronary segments analyzed. Reendothelialization was also analyzed, which was complete, with 100% of endothelial lining recovered at 28 days after stent implantation, in PAP-1 and control treatment groups. Likewise, in the transplant vasculopathy model, endothelial lining was also present in 100% of the luminal surface of the allografts treated with PAP-1, without any differences with respect to polymer-treated allografts or autografts, demonstrating that neither PAP-1 nor the polymer had any deleterious effect on endothelial cell proliferation. A limitation of the in-stent-restenosis model used in the present study is the fact that stent implantation was performed in healthy coronary arteries. It is possible that a large preclinical model involving stent implantation in previously atheromatous arteries would have different results, which could be interesting to analyze in future studies.

In summary, our work demonstrates Kv1.3 modulation is a potential therapeutic approach for cardiovascular diseases related to intimal hyperplasia development. Technical issues beyond our capacity may be held responsible for the lack of benefit in the in-stent restenosis model, most likely due to insufficient release of active drug. Given all our previous and present evidence regarding the beneficial effects of Kv1.3 inhibition with PAP-1, further studies are granted to analyze the optimal conditions in which this promising compound could be used in the clinical context.

Acknowledgments

We thank Nadia Castillo (IDIBAPS, Hospital Clínic, Barcelona) and Esperanza Alonso (IBGM, Valladolid) for excellent technical assistance. Part of this work was developed at the *Centre de Recerca Biomèdica Cellex*, Barcelona.

This work was supported by a Translational Research Project on Cardiology (2015) of the *Sociedad Española de Cardiología* and *Fondo de Investigación Sanitario Instituto de Salud Carlos III* (PI11/00225) to M. Roqué; BFU2016-75360-R from the *Ministerio de Economía y Competitividad* (MINECO) to M.T. Pérez-García and J.R. López-López; *Junta de Castilla y León* Grant VA114P17 to M.T. Pérez-García; and the CERCA Programme of the *Generalitat de Catalunya*.

All authors have read the policy on disclosure of potential conflicts and have no competing interests to declare. All authors have read the journal's authorship agreement and approved the final version of the manuscript.

References

1. Mulvany M. Vascular remodelling of resistance vessels: can we define this? *Cardiovasc Res*. 1999;41(1):9-13. doi:10.1016/S0008-6363(98)00289-2
2. Owens GK, Kumar MS, Wamhoff BR. Molecular Regulation of Vascular Smooth Muscle Cell Differentiation in Development and Disease. *Physiol Rev*. 2004;84(3):767-801. doi:10.1152/physrev.00041.2003
3. Wamhoff BR, Bowles DK, Owens GK. Excitation–Transcription Coupling in Arterial Smooth Muscle. *Circ Res*. 2006;98(7):868-878. doi:10.1161/01.RES.0000216596.73005.3c
4. Pérez-García MT, Cidad P, López-López JR. The secret life of ion channels: Kv1.3 potassium channels and proliferation. *Am J Physiol Physiol*. 2018;314(1):C27-C42. doi:10.1152/ajpcell.00136.2017
5. Tsutsui H, Ziada KM, Schoenhagen P, et al. Lumen Loss in Transplant Coronary Artery Disease Is a Biphasic Process Involving Early Intimal Thickening and Late Constrictive Remodeling. *Circulation*. 2001;104(6):653-657. doi:10.1161/hc3101.093867
6. Valantine HA. Cardiac allograft vasculopathy: central role of endothelial injury leading to transplant "atheroma." *Transplantation*. 2003;76(6):891-899. doi:10.1097/01.TP.0000080981.90718.EB
7. Costello JP, Mohanakumar T, Nath DS. Mechanisms of chronic cardiac allograft rejection. *Texas Hear Inst J*. 2013;40(4):395-399.
8. Bennett MR, O'Sullivan M. Mechanisms of angioplasty and stent restenosis: implications for design of rational therapy. *Pharmacol Ther*. 2001;91(2):149-166. doi:10.1016/S0163-7258(01)00153-X
9. Piek JJ, Van Der Wal AC, Meuwissen M, et al. Plaque inflammation in restenotic coronary lesions of patients with stable or unstable angina. *J Am Coll Cardiol*. 2000;35(4):963-967. doi:10.1016/S0735-1097(99)00647-6
10. Farb A, Weber DK, Kolodgie FD, Burke AP, Virmani R. Morphological Predictors of Restenosis After Coronary Stenting in Humans. *Circulation*. 2002;105(25):2974-2980.

doi:10.1161/01.CIR.0000019071.72887.BD

11. Urrego D, Tomczak AP, Zahed F, Stühmer W, Pardo LA. Potassium channels in cell cycle and cell proliferation. *Philos Trans R Soc B Biol Sci*. 2014;369(1638):20130094. doi:10.1098/rstb.2013.0094

12. Wonderlin WF, Strobl JS. Potassium Channels, Proliferation and G1 Progression. *J Membr Biol*. 1996;154(2):91-107. doi:10.1038/237116a0

13. Joseph BK, Thakali KM, Moore CL, Rhee SW. Ion channel remodeling in vascular smooth muscle during hypertension: Implications for novel therapeutic approaches. *Pharmacol Res*. 2013;70(1):126-138. doi:10.1016/j.phrs.2013.01.008

14. Lang F, Föller M, Lang K, et al. Cell Volume Regulatory Ion Channels in Cell Proliferation and Cell Death. In: *Methods in Enzymology*. Vol 428. ; 2007:209-225. doi:10.1016/S0076-6879(07)28011-5

15. Cheong A, Li J, Sukumar P, et al. Potent suppression of vascular smooth muscle cell migration and human neointimal hyperplasia by KV1.3 channel blockers. *Cardiovasc Res*. 2011;89(2):282-289. doi:10.1093/cvr/cvq305

16. Cidad P, Moreno-Domínguez A, Novensá L, et al. Characterization of Ion Channels Involved in the Proliferative Response of Femoral Artery Smooth Muscle Cells. *Arterioscler Thromb Vasc Biol*. 2010;30(6):1203-1211. doi:10.1161/ATVBAHA.110.205187

17. Cidad P, Novensà L, Garabito M, et al. K+ Channels Expression in Hypertension After Arterial Injury, and Effect of Selective Kv1.3 Blockade with PAP-1 on Intimal Hyperplasia Formation. *Cardiovasc Drugs Ther*. 2014;28(6):501-511. doi:10.1007/s10557-014-6554-5

18. Ray JL, Leach R, Herbert JM, Benson M. Isolation of vascular smooth muscle cells from a single murine aorta. *Methods Cell Sci*. 2001;23(4):185-188. doi:10.1023/A:1016357510143

19. Livak KJ, Schmittgen TD. Analysis of Relative Gene Expression Data Using Real-Time Quantitative PCR and the 2−ΔΔCT Method. *Methods*. 2001;25(4):402-408.

doi:10.1006/meth.2001.1262

20. Miguel-Velado E, Moreno-Domínguez A, Colinas O, et al. Contribution of Kv Channels to Phenotypic Remodeling of Human Uterine Artery Smooth Muscle Cells. *Circ Res*. 2005;97(12):1280-1287. doi:10.1161/01.RES.0000194322.91255.13

21. Rigol M, Solanes N, Sionis A, et al. Effects of Cyclosporine, Tacrolimus and Sirolimus on Vascular Changes Related to Immune Response. *J Hear Lung Transplant*. 2008;27(4):416-422. doi:10.1016/j.healun.2008.01.006

22. Solanes N, Rigol M, Khabiri E, et al. Effects of cryopreservation on the immunogenicity of porcine arterial allografts in early stages of transplant vasculopathy. *Cryobiology*. 2005;51(2):130-141. doi:10.1016/j.cryobiol.2005.06.006

23. Rigol M, Solanes N, Roura S, et al. Allogeneic adipose stem cell therapy in acute myocardial infarction. *Eur J Clin Invest*. 2014;44(1):83-92. doi:10.1111/eci.12195

24. Perez de Prado A, Perez-Martinez C, Cuellas C, et al. Preclinical Evaluation of Coronary Stents: Focus on Safety Issues. *Curr Vasc Pharmacol*. 2013;11(1):74-99. doi:10.2174/157016113804547575

25. Schwartz RS, Huber KC, Murphy JG, et al. Restenosis and the proportional neointimal response to coronary artery injury: Results in a porcine model. *J Am Coll Cardiol*. 1992;19(2):267-274. doi:10.1016/0735-1097(92)90476-4

26. Kornowski R, Hong MK, Tio FO, Bramwell O, Wu H, Leon MB. In-Stent Restenosis: Contributions of Inflammatory Responses and Arterial Injury to Neointimal Hyperplasia. *J Am Coll Cardiol*. 1998;31(1):224-230. doi:10.1016/S0735-1097(97)00450-6

27. Suzuki T, Kopia G, Hayashi S-I, et al. Stent-Based Delivery of Sirolimus Reduces Neointimal Formation in a Porcine Coronary Model. *Circulation*. 2001;104(10):1188-1193. doi:10.1161/hc3601.093987

28. Kotecha SA, Schlichter LC. A Kv1.5 to Kv1.3 Switch in Endogenous Hippocampal Microglia and a Role in Proliferation. *J Neurosci*. 1999;19(24):10680-10693. doi:10.1523/JNEUROSCI.19-24-10680.1999

29. Cidad P, Miguel-Velado E, Ruiz-McDavitt C, et al. Kv1.3 channels modulate human

vascular smooth muscle cells proliferation independently of mTOR signaling pathway. *Pflügers Arch - Eur J Physiol*. 2015;467(8):1711-1722. doi:10.1007/s00424-014-1607-y

30. Arévalo-Martínez M, Cidad P, García-Mateo N, et al. Myocardin-Dependent Kv1.5 Channel Expression Prevents Phenotypic Modulation of Human Vessels in Organ Culture. *Arterioscler Thromb Vasc Biol*. 2019;39(12):E273-E286. doi:10.1161/ATVBAHA.119.313492

31. Chen Y-J, Lam J, Gregory CR, Schrepfer S, Wulff H. The Ca2+-Activated K+ Channel KCa3.1 as a Potential New Target for the Prevention of Allograft Vasculopathy. Attali B, ed. *PLoS One*. 2013;8(11):e81006. doi:10.1371/journal.pone.0081006

32. Schwartz RS, Edelman E, Virmani R, et al. Drug-Eluting Stents in Preclinical Studies. *Circ Cardiovasc Interv*. 2008;1(2):143-153. doi:10.1161/CIRCINTERVENTIONS.108.789974

Figure Legends

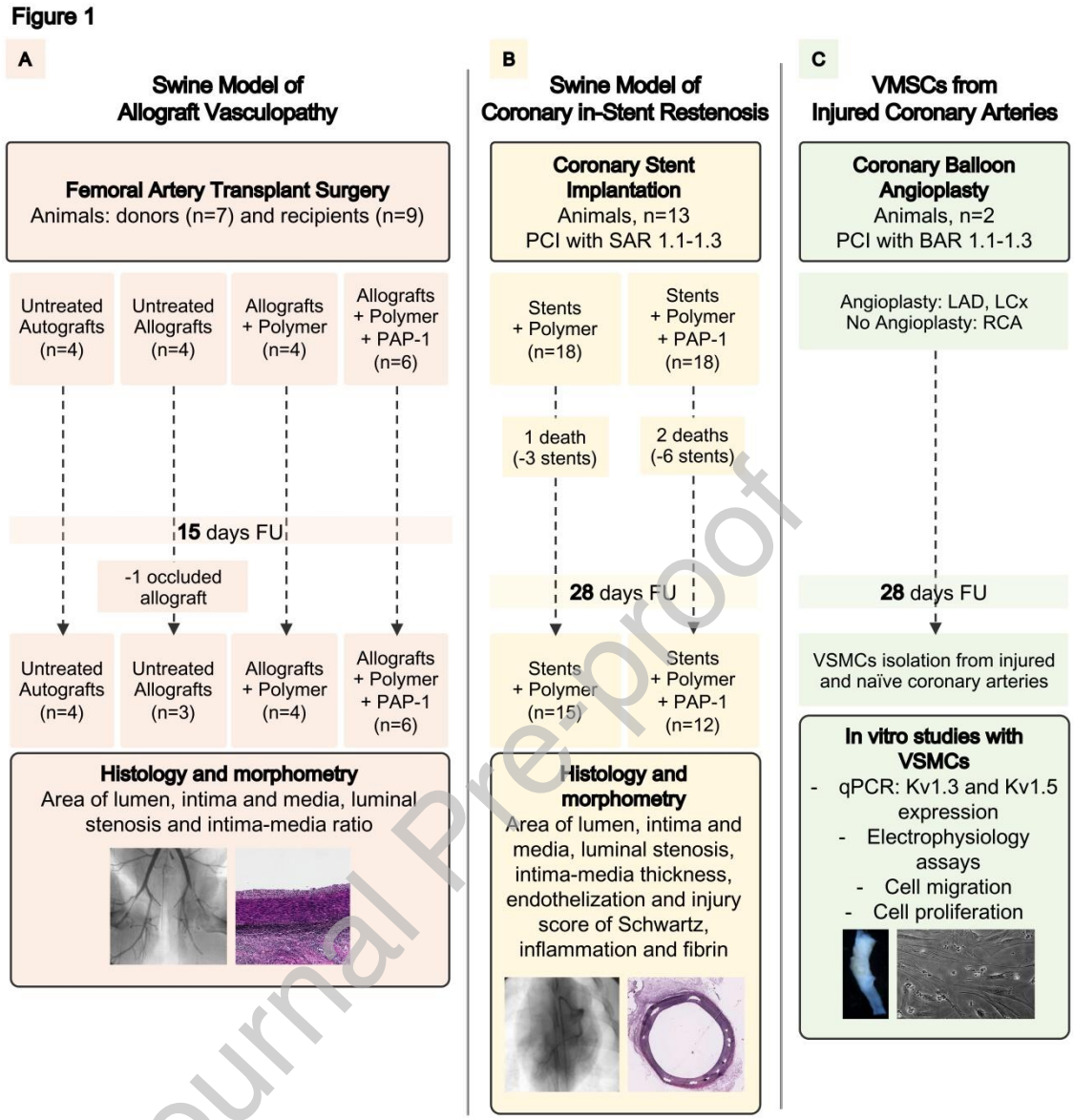

Figure 1. Study design

Flow charts illustrating the design of *in vitro* studies with VSMCs obtained from injured and naïve coronary arteries from pigs (panel **A).** The number of animals used and studied in the swine models of allograft vasculopathy and coronary in-stent restenosis are described in panels **B** and **C**, respectively. BAR indicates balloon-to-artery ratio; FU, follow-up; LAD, left anterior descending coronary artery; LCx, left circumflex coronary artery; PCI, percutaneous coronary intervention; RCA, right coronary artery; SAR, stent-to-artery ratio; VSMCs, vascular smooth muscle cells.

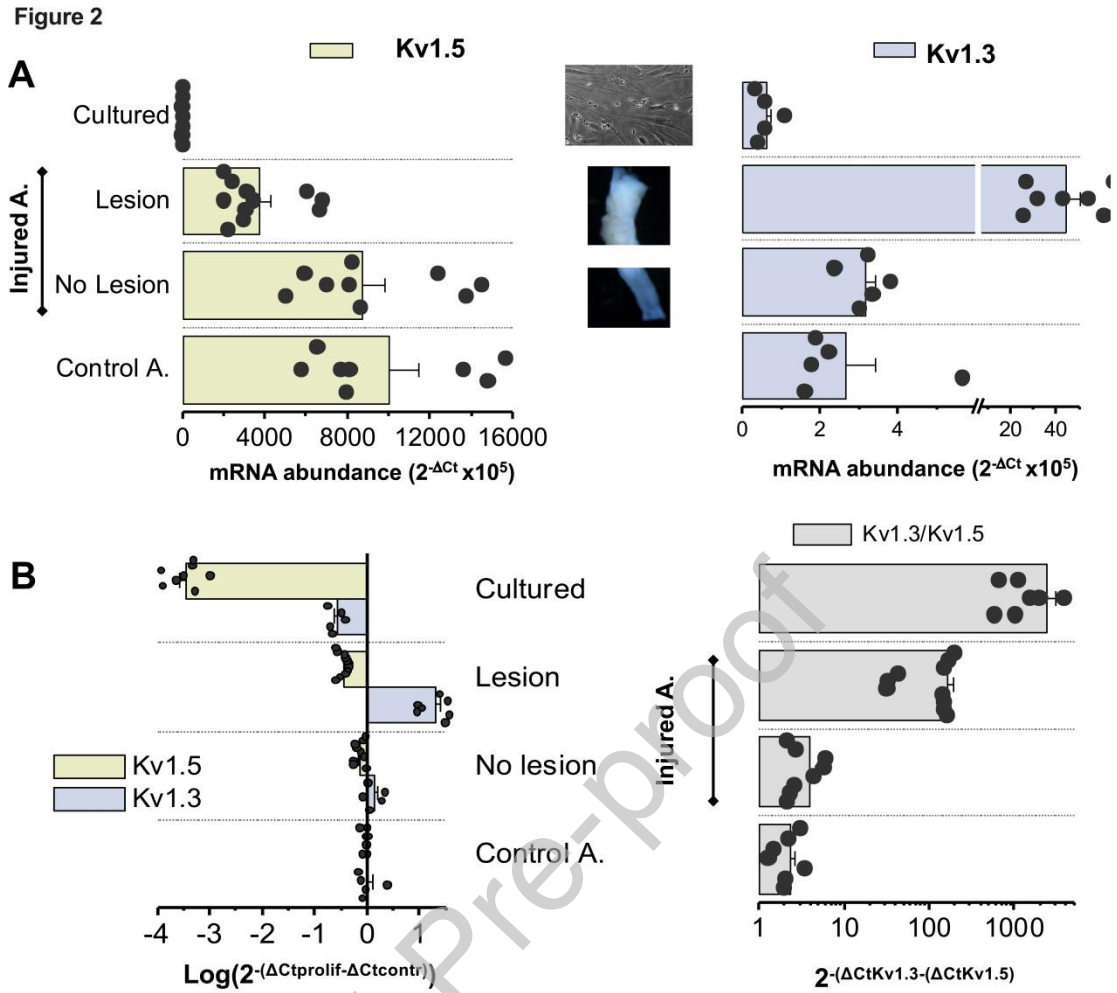

Figure 2. Changes in expression of Kv1.3 and Kv1.5 mRNA upon phenotypic modulation of pig coronary VSMCs

A. Relative mRNA abundance of the Kv1.5 (left) and Kv1.3 (right) channel genes in contractile and proliferating VSMC from pig coronary arteries. Each bar is the mean of 5-7 determinations obtained in at least 3 duplicate assays. **B.** The left panel shows differential mRNA expression of Kv1.3 and Kv1.5 in cultured VSMC and injured and control porcine coronary arteries. The changes in expression between the different experimental conditions were calculated from 2(-ΔΔCt), using control arteries (control A) as calibrator. Note the log scale. Each bar is the mean ± SEM of 10 determinations. The bars plot on the right shows the Kv1.3:Kv1.5 ratio expressed as $2^{-\Delta\Delta Ct}$, where ΔΔCt was ΔCtKv1.3–ΔCtKv1.5. There is a progressive increase of this ratio associated to VSMCs dedifferentiation. Each data point was obtained from 3-5 independent determinations in triplicate.

Figure 3

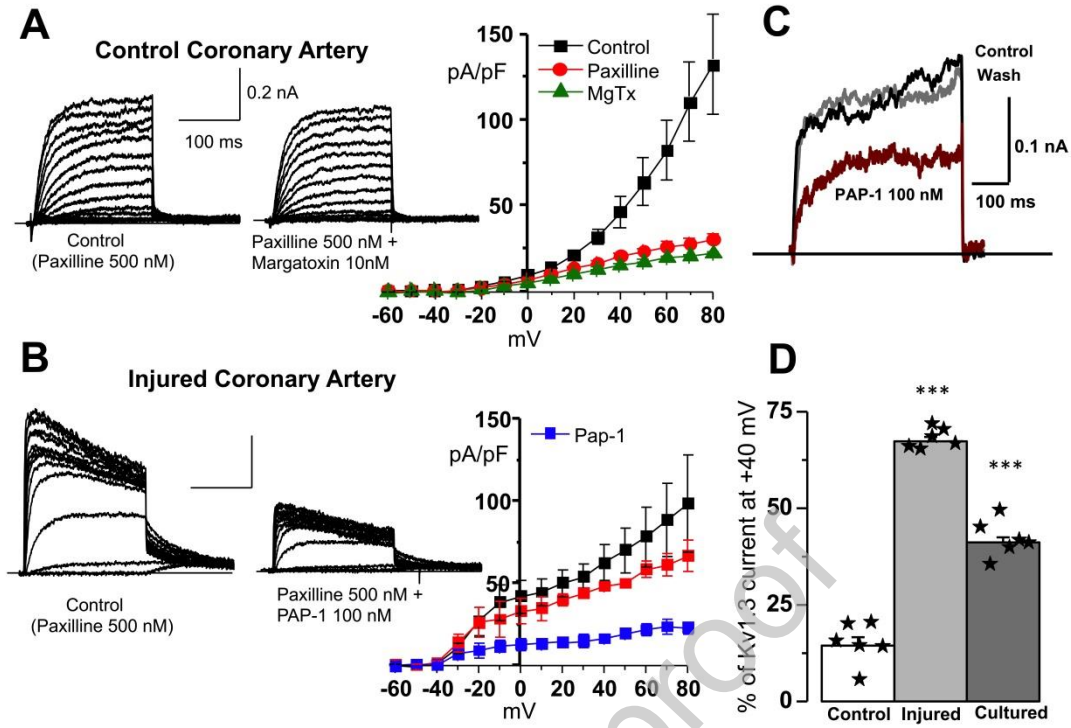

Figure 3. Functional expression of Kv1.3 currents in pig coronary VSMCs

A. Current traces obtained in freshly dissociated VSMCs from a control coronary artery. Traces were elicited by 200 ms pulses from -60 to +80 mV in 10 mV steps. Kv currents were obtained after BKCa block with 500 nM paxilline (left traces). The effect of Margatoxin (10 nM) in this same cell is also shown. The right panel shows the average current-voltage relationship obtained with this protocol by plotting the peak current amplitude against the pulse potential. Each point is the Mean ± SEM, n=5. **B.** A similar experiment carried out in a freshly dissociated VSMCs from an injured coronary artery, in this case showing the effect of 100 nM PAP-1. The I/V curves on the right are the average of 6 cells from 2 different experiments. **C.** Representative traces obtained in 500 ms pulses from a holding potential of -60mV to +40mV in a cultured VSMC in control conditions, upon application of PAP-1 (100nM) and after washing again with control solution. **D.** The bar plot shows the fraction of Kv1.3 current (defined as the 10 nM MgTx or 100nM PAP-1 sensitive current) in the total Kv current recorded in pulses to +40mV in freshly dispersed VSMCs from control arteries, (white bar), and from injured arteries (clear grey bar) and cultured VSMCs (dark grey bar). Data are mean ± SEM of 5-7 cells in each group.

***p<0.001 as compared to control. The main effects are compared, when indicated, by ANOVA followed by Bonferroni post-hoc test.

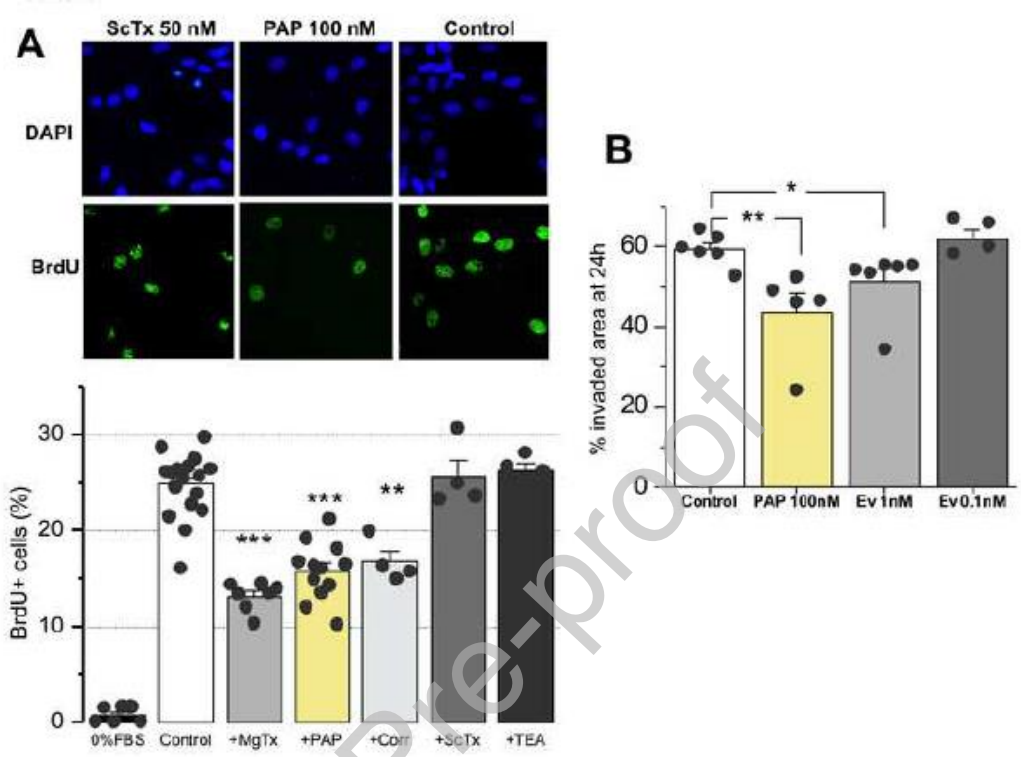

Figure 4. Effect of Kv1.3 blockade on pig coronary VSMC proliferation and migration

A. Proliferation rate was calculated as the percentage of cells incorporating BrdU. Each bar is mean ± SEM of 6-15 independent experiments from at least four different cultures. Representative images in three of the experimental conditions tested are shown in the upper panels. ** p<0.01; ***p<0.001 as compared to control. The main effects are compared, when indicated, by ANOVA followed by Bonferroni post-hoc test. **B.** Effect of Kv1.3 blockade or mTOR blockade on pig coronary VSMC migration calculated as the percentage of invaded area in scratch assays. Each bar is the mean ± SEM of 5-6 independent experiments carried out in 3 different VSMC cultures. Ev indicates everolimus. * p<0.05; **p<0.01 as compared to control. The main effects are compared, when indicated, by ANOVA followed by Bonferroni post-hoc test.

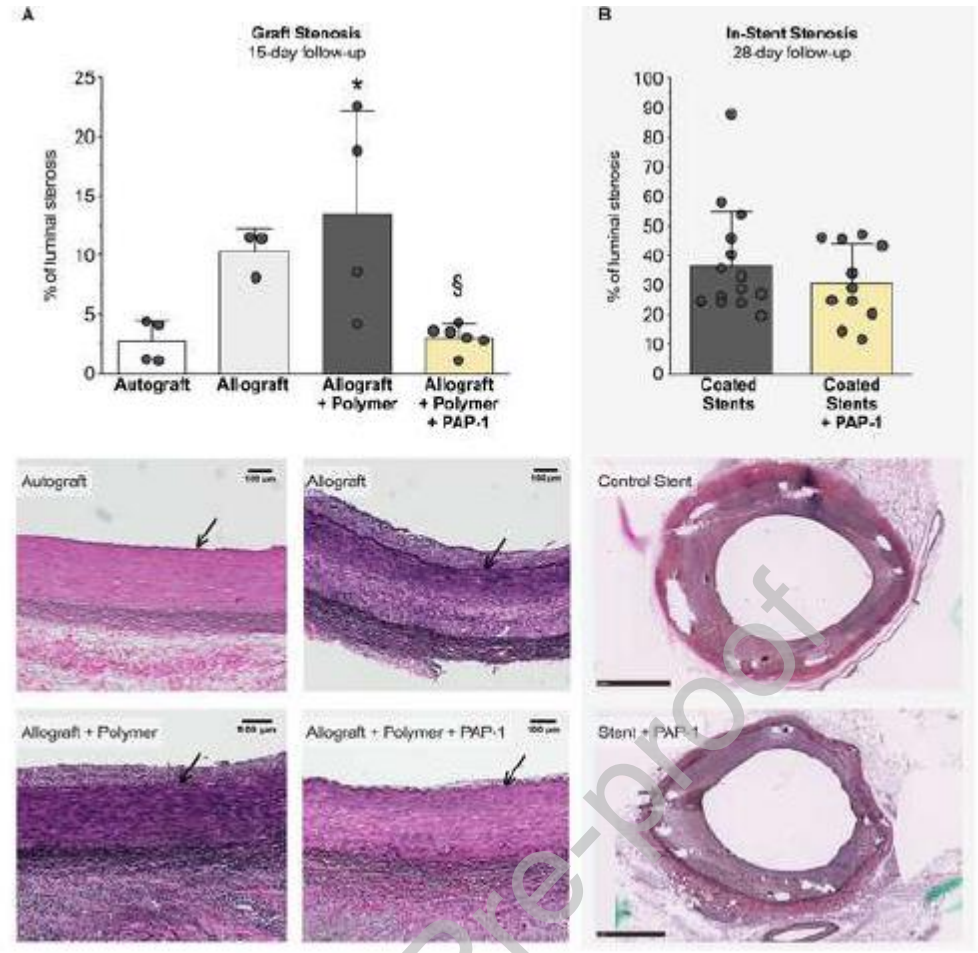

Figure 5. Effect of Kv1.3 inhibition with PAP-1 on Porcine Models of Allograft Vasculopathy and Coronary In-Stent Restenosis

A. Superior: Bar graph representing mean ± SEM of percentage of luminal stenosis of untreated autograft (n=4); untreated allograft (n=3); polymer-treated allograft (n=4); and polymer+PAP-1-treated allograft (n=6). Inferior: Representative photomicrographs of femoral artery cross-sections 15 days after transplantation. Verhoeff Van Gieson stain. Original magnification: x100. Arrows indicate internal elastic lamina. * $p<0.05$ vs untreated autografts; § $p<0.05$ vs polymer treated allografts. **B.** Superior: Bar graph representing mean ± SEM of percentage of luminal stenosis of control (n=15) and PAP-1-eluting coronary stents (n=12). Inferior: Representative photomicrographs of stented coronary segments cross-sections at 28-day follow-up. Verhoeff Van Gieson stain. Original magnification: 10x. Differences were studied with the t test.

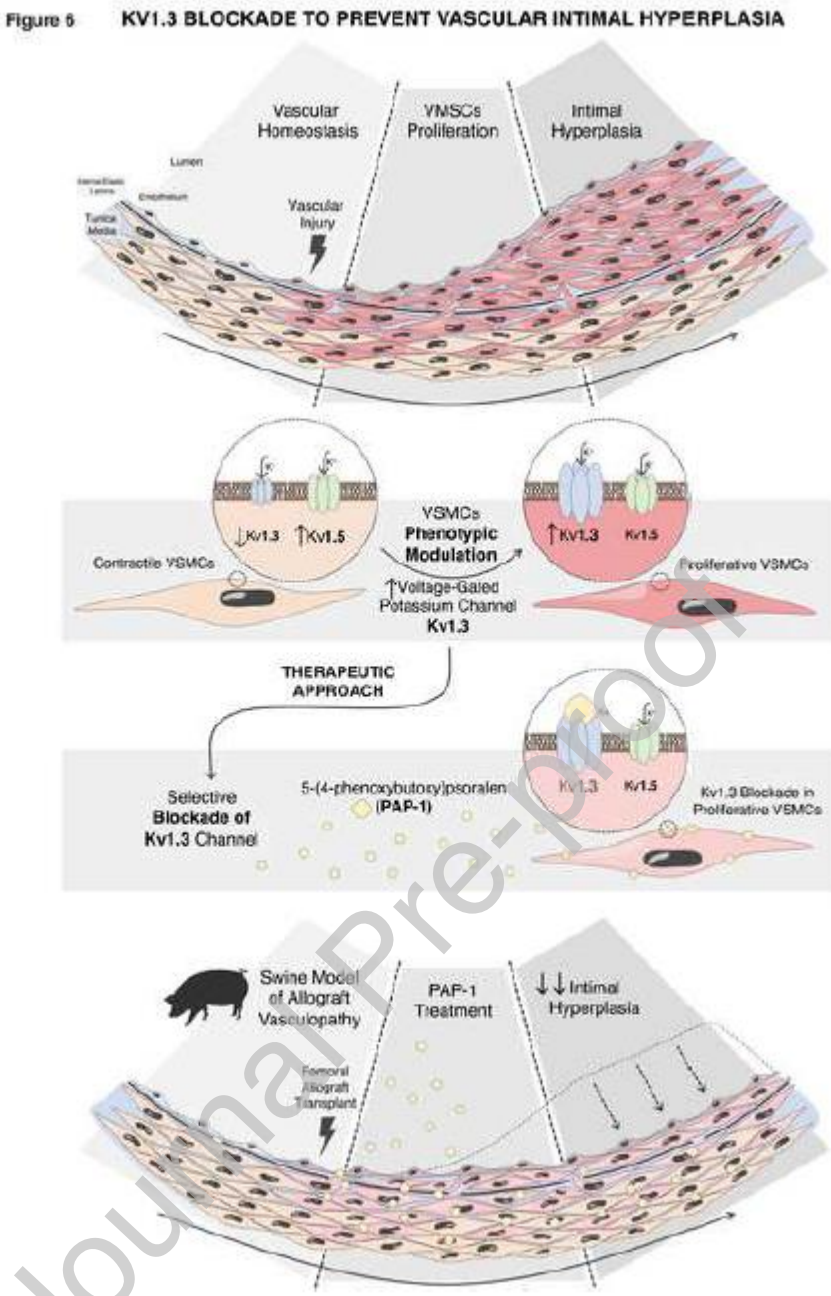

Figure 6. Main Findings

A shift in Kv1.3/1.5 channels expression is observed in the phenotypic modulation of VMSCs after vascular damage. The elective blockade of Kv1.3 channels inhibit intimal proliferation in a swine model of artery allograft vasculopathy.

Table 1. Morphometric analysis of femoral artery grafts

	Total area (mm^2)	Medial area (mm^2)	Intimal area (mm^2)	Luminal area (mm^2)	Luminal stenosis (%)	Intima-media ratio
Untreated Autografts (n=4)	11.46±4.01	3.98±1.33	0.14±0.09	6.09±3.33	2.72±1.79	0.03±0.01
Untreated Allografts (n=3)	13.47±2.16	3.57±0.26	0.83±0.29*	7.08±1.45	10.32±1.92	0.23±0.06*#
Polymer Treated Allografts (n=4)	10.19±5.73	3.26±0.77	0.41±0.19	5.00±4.90	13.54±8.59*	0.12±0.04*
Polymer+PAP-1 Treated Allografts (n=6)	13.57±9.01	3.88±2.13	0.21±0.14**	7.62±5.75	3.06±1.08#	0.05±0.01**
ANOVA (P value)	0.850	0.902	**0.001**	0.834	**0.006**	**<0.001**

Bonferroni's post hoc tests *p < 0.05 vs untreated autografts; **p ≤ 0.05 vs untreated allografts;

# p < 0.05 vs polymer treated allografts.

Table 2. Morphometric Analysis of the Coronary Stented Arteries

	Control (n=15)	PAP-1 (n=12)	P value
Neointimal area (mm^2)	1.75±1.16	1.50±0.56	0.499
Area of media	1.66±1.20	1.43±0.37	0.546
Intima-media thickness	3.41±2.05	2.92±0.78	0.458
Area of stenosis (%)	36.90±18.23	31.01±13.08	0.372
Endothelial area (%)	99.47±1.13	99.55±1.51	0.879
Endothelization >95%	100% (15/15)	100% (12/12)	-
Injury score of Schwartz	0.79±0.43	0.68±0.53	0.560
Injury score of Schwartz ≥1	20% (3/15)	27.27% (3/12)	0.678
Inflammation score	1.11±0.70	1.07±0.71	0.904
Inflammation score ≥1	53.33% (8/15)	45.45% (5/12)	0.705
Fibrin score	0.29±0.38	0.21±0.34	0.598
Fibrin score ≥1	13.33% (2/15)	9.09% (1/12)	0.750

P values from *t* test.

Translational Significance

Intimal hyperplasia formation, in response to vascular injury, entails ischemia and risk of myocardial infarction and graft failure, among other clinical entities. This pathological process is still associated to high socio-economic costs despite recent therapeutic advances. Using two clinically-relevant animal models of vascular intimal proliferation, from a translational point of view, we assessed the effect of PAP-1, a Kv1.3 selective channel blocker, to reduce intimal hyperplasia. Our results demonstrate the therapeutic potential of PAP-1 to avoid intimal proliferation on chronic allograft vasculopathy, a critical aspect of solid organs transplantation.